Surface morphology and magnetic anisotropy in (Ga,Mn)As

S. Piano,[1] X. Marti,[2] A. W. Rushforth,[1] K. W. Edmonds,[1] R. P. Campion,[1] M. Wang,[1] O. Caha,[3] T. U. Schülli,[4] V. Holý,[2] and B. L. Gallagher[1]

[1]*School of Physics and Astronomy, University of Nottingham, University Park, Nottingham, NG7 2RD, United Kingdom.*

[2]*Department of Condensed Matter Physics, Faculty of Mathematics and Physics, Charles University, Ke Karlovu 5, 121 16 Prague 2, Czech Republic.*

[3]*Institute of Condensed Matter Physics, Faculty of Science, Masaryk University, Kotlářská 2, 611 37 Brno, Czech Republic.*

[4]*ESRF, BP220 Grenoble, France.*

Atomic Force Microscopy and Grazing incidence X-ray diffraction measurements have revealed the presence of ripples aligned along the $[1\bar{1}0]$ direction on the surface of (Ga,Mn)As layers grown on GaAs(001) substrates and buffer layers, with periodicity of about 50 nm in all samples that have been studied. These samples show the strong symmetry breaking uniaxial magnetic anisotropy normally observed in such materials. We observe a clear correlation between the amplitude of the surface ripples and the strength of the uniaxial magnetic anisotropy component suggesting that these ripples might be the source of such anisotropy.

PACS numbers: 75.50.Pp, 75.30.Gw, 07.79.Lh, 61.05.cp

The ferromagnetic semiconductor (Ga,Mn)As has been the subject of intense research due to its potential application in spintronic devices and quantum computation[1,2]. The ferromagnetic interaction between the local Mn moments is mediated by the itinerant holes giving rise to a strong sensitivity of the magnetic properties on the carrier density and lattice strain[3,4]. Developing an understanding of how these interactions give rise to the magnetic properties is essential in order to realise the applications of the (Ga,Mn)As compound. The p-d Zener model gives a satisfactory explanation for several of the properties. For instance, (Ga,Mn)As grown epitaxially on GaAs experiences a compressive which gives rise to a magnetic anisotropy with the easy axis in the plane of the layer, consistent with the predictions of the model[3,4]. In addition, the in plane magnetic anisotropy is found ubiquitously to consist of a cubic contribution, favouring easy axes along the [100] directions, and a uniaxial component favouring one of the [110] directions[5,6]. The presence of the cubic component is consistent with the symmetry of the GaAs lattice, but the microscopic origin of the uniaxial component has not yet been explained. Several theoretical studies have invoked the concept of a uniform anisotropic strain of order 10^{-4} to account for the uniaxial anisotropy component[4,5,7], but no direct experimental evidence of such a lattice distortion has been reported[8].

In this paper we show experimental evidence, from Atomic Force Microscopy (AFM) and Grazing incidence X-ray diffraction (GID) measurements, of the presence of periodic ripples in (Ga,Mn)As layers grown on GaAs. The analysis of AFM and GID measurements have evidenced a period of these ripples of about 50 nm. We observe a clear correlation between the magnitude of the uniaxial anisotropy and the amplitude of the surface ripples.

(Ga,Mn)As films with thicknesses (t), $5nm$, $7nm$ and $25nm$, and Mn concentrations, 6% and 12%, have been deposited on GaAs (100) substrates by low temperature ($\sim 200°C$) molecular beam epitaxy on 100nm thick low temperature or high temperature ($\sim 580°C$) GaAs and AlGaAs

buffer layers. Atomic force microscopy (AFM) images were obtained by using an Asylum Research MFP-3D atomic force microscope. Before performing the measurements the samples were cleaned with a 1:3 HCl:H_2O solution to remove the superficial oxide layer. Measurements on uncleaned samples have shown the same surface structures but with additional surface contamination indicating that the cleaning was not modifying the surface morphology. The images were taken on 1x1 μm^2 areas along two different crystallographic directions, $[1\bar{1}0]$ and [110]. Grazing incidence X-ray diffraction (GID) measurements were performed at the beamline ID01 of the ESRF in Grenoble (France) using a photon energy of 6.5 keV and a linear detector mounted perpendicular to the sample surface. Magnetometry measurements on the as-grown films were carried out using a Quantum Design Superconducting Quantum Interference Device (SQUID) magnetometer.

Fig. 1 shows the remnant magnetisation measured along the $[1\bar{1}0]$ and [110] directions for one of our samples. Consistent with previous studies of unannealed (Ga,Mn)As layers we find that all samples within our study have a dominant in plane $[1\bar{1}0]$ uniaxial magnetic easy axis at high temperature, with competition between in plane $[1\bar{1}0]$ uniaxial and in-plane [100] bi-axial easy axes at low temperatures. We consider a phenomenological description of the free energy in terms of cubic (K_C) and uniaxial (K_U) anisotropy constants:
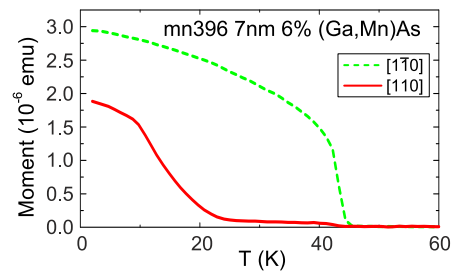

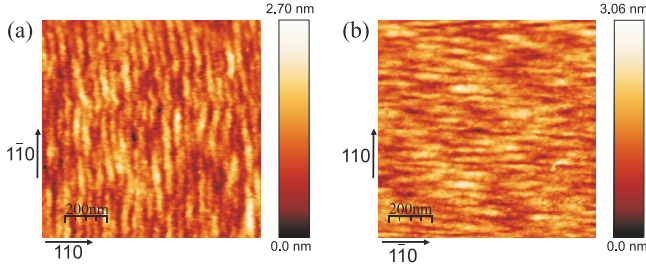FIG. 1. Temperature dependence of the remnant magnetisation along [110] and $[1\bar{1}0]$ direction.

FIG. 2. AFM image of the sample Mn 381 a) along [110] direction, and b) along [1$\bar{1}$0] direction.

$$E = K_C \sin^2(\theta)\cos^2(\theta) + K_U \sin^2(\theta) - MsH\cos(\theta - \theta_0),$$

where θ and θ_0 measure the direction of the magnetisation and the external magnetic field with respect to the [110] crystal direction. By minimising this expression for the energy it can be shown that the relative strength of the uniaxial to cubic anisotropy $K_U/K_C = \cos 2[\tan^{-1}(M_{1\bar{1}0}/M_{110})]$, where $M_{1\bar{1}0}$ and M_{110} represent the components of the magnetisation measured along [1$\bar{1}$0] and [110] respectively. We find that the temperature-dependence of the remnant magnetization after field cooling in all the studied samples is generally well-described by this phenomenological model.

Fig. 2 shows AFM images along the [1$\bar{1}$0] and [110] directions for a 7nm thick (Ga,Mn)As sample containing 6% Mn (sample Mn381). The images clearly reveal the presence of ripples aligned along the [1$\bar{1}$0] direction. Ripple patterns such as these are known to form during the MBE growth of low temperature ($< 260°$C) GaAs in the presence of excess As. The mechanism causing the ripples to form is the suppression of diffusion of adatoms at step edges. The excess As in ref.[9] was believed to act as a surfactant aiding the diffusion of adatoms along the step edges. For our samples, which are

not grown with a significant excess of As, we believe that Mn deposited at the surface may be playing a similar role as a surfactant. Similar ripple patterns are observed in the images obtained for all the samples in our study. We have used Fourier analysis to extract quantitative information from these images. We can define the power spectral density as $p_s = |\phi_s|^2$, where ϕ_s is the Fourier amplitude corresponding to a (dimensionless) frequency $f_s = s - 1$.

The mean frequency, $\overline{f}(y)$, per line is then obtained as the average of the frequencies of all Fourier harmonics (along a given scan line) weighted with the corresponding power spectral densities: $\overline{f}(y) = \left[\sum_{s=1}^{n/2}(s-1)p_s\right]/\left[\sum_{s=1}^{n/2}p_s\right]$. Then, the global 'effective' mean-frequency ($\overline{f}$), characterising the oscillations in the whole image, is given by the mean $\overline{f}(y)$ of each line along all horizontal scan lines and the associated error is its standard deviation. From the $\overline{f}$ and L (the width of the image) we obtain the 'effective' period of the oscillations: $\tau = L/\overline{f}$. Such an effective period is used to give a quantitative measure of the periodicity of the ripples observed on the AFM image. In addition, the root mean square (RMS) roughness of each image in the direction perpendicular to the ripples is calculated by taking the standard deviation of the height for each line scan and averaging this over the whole image.

The ripples are found to be present in all of the (Ga,Mn)As samples studied. In Fig. 3 we plot K_U/K_C from SQUID magnetometry measurements at 2K versus the RMS roughness, and in Table I we tabulate the data for each sample. In order to distinguish the effect of the roughness from effects which may alter the absolute value of K_C we compare the samples within groups of similar thickness, nominal Mn concentration and Curie temperature. We find that for each group of samples there is a clear relation between the ratio of the magnetic anisotropy constants K_U/K_C and the RMS roughness, in particular the influence of the uniaxial anisotropy increases as the RMS roughness increases.

In order to obtain information on the periodicity of the nanostructures over the whole sample surface, grazing incidence X-ray diffraction (GID) measurements were also performed on one sample (Mn 381). In the GID geometry, both the angle of incidence (α_i) and the exit angle (α_f) of the x-ray beams are close to the critical angle(α_c) of total external reflection ($0.38°$ for the energy used) thus leading to a large footprint illuminating the sample surface, after the aperture

sample	t , Mn%	buffer	τ	RMS	K_u/K_c
Mn 352	5, 6%	A HT	49.7 ± 12.7	0.35±0.07	0.241
Mn 536	5, 6%	B HT + B LT	45.5 ± 11.3	0.31±0.04	0.157
Mn 396	7, 6%	B HT	47.7 ± 8.2	0.48±0.06	0.498
Mn 381	7, 6%	B HT	41.9 ± 6.4	0.38±0.04	0.325
Mn 555	7, 6%	A HT	47.7 ± 6.3	0.3±0.1	0.158
Mn 535	7, 6%	B LT	45.4 ± 10.3	0.34±0.04	0.089
Mn 394	7, 6%	A HT	59.8 ± 13.5	0.35±0.05	0.249
Mn 437	25, 12%	A LT	51.5 ± 8.6	0.36 ± 0.06	0.113
Mn 438	25, 12%	A LT	61.7 ± 11.4	0.37 ±0.07	0.149
Mn 554	25, 6%	B LT	56.0 ± 16.9	0.35 ± 0.04	0.039
Mn 499	25, 6%	A HT	47.8 ± 11.8	0.31± 0.05	0.018
Mn 330	25, 6%	A HT	65.9 ± 11.3	0.31 ± 0.09	0.107
Mn 490	25, 6%	A HT	52.5 ± 8.3	0.28 ± 0.03	-0.005

TABLE I. For each sample the thickness (t) in nm, the Mn concentration (Mn %), the buffer layer (A: GaAs; B: AlGaAs; HT: high temperature; LT: low temperature), the period (τ) in nm, the RMS roughness in nm and the magnetic anisotropy coefficient (K_U/K_C), are shown.
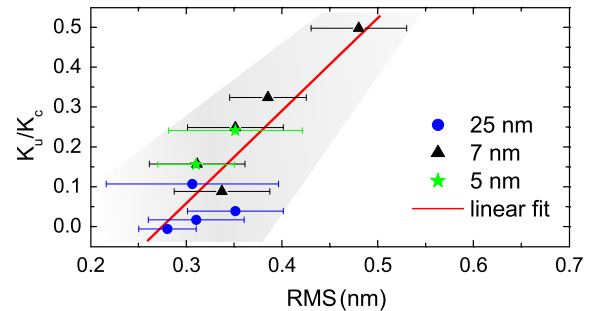

FIG. 3. The magnetic anisotropy coefficient, K_U/K_C as a function of the total RMS roughness for samples with 6% of Mn.

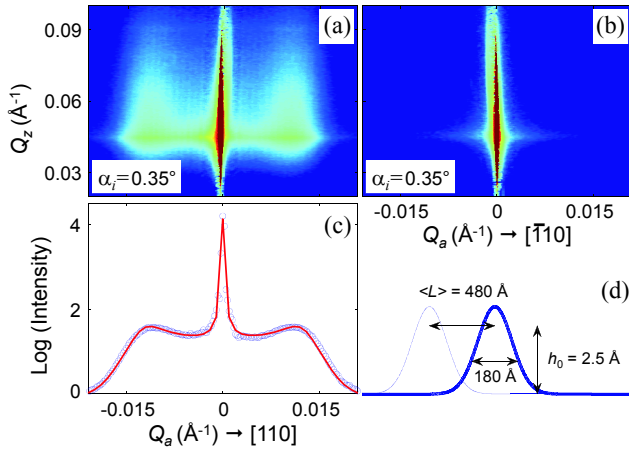FIG. 4. Transverse GID scans for sample Mn381 collected along two perpendicular directions at $\alpha_i = 0.35°$. While the scans with the primary beam directed across the ripples (a) show two symmetric satellites denoting a periodicity of 48 nm, such satellites are absent in the scans along the ripples (b). (c) Profile from data in panel (a) and a fit assuming Gaussian-shaped ripples are shown by circles and solid line, respectively. (d) Sketch of the dimensions of the ripples.

of horizontal slits, up to a few millimeters. The difference in the azimuthal directions of the beams was set close to $2\theta_B$, where θ_B is the Bragg angle[10]. In particular, two in-plane diffraction vectors $h = 220$ (perpendicular to the ripples), and $h = \bar{2}20$ (parallel to the ripples) were investigated and, for each diffraction, we measured two reciprocal-space distributions of the scattered intensity in the reciprocal planes Q_aQ_z and Q_aQ_z, where Q_aQ_z is the component of the scattering vector Q perpendicular to the surface, and Q_a is the angular component of Q perpendicular to h. The angular map in Fig. 4 (a) taken in the diffraction $\bar{2}20$ exhibits two side maxima (intensity satellites). Since Q_a in this map is parallel to [110], i.e. perpendicular to the ripples, these maxima stem from the periodicity of the ripples and the satellite distance is inversely proportional to the ripple period τ. In turn, the width of the satellites depends on the root-mean-square deviation of the ripple spacing σ_τ. From the intensity map we extracted the intensity integrated over Q_z and compared it to a theoretical model. In the model, we assumed that the ripple sequence obeys the standard one-dimensional short-range order model[12] and that the shape of a cross-section of a single ripple is Gaussian: $h(x) = h_0 \exp(-x^2/R^2)$.

From Fig. 4(c) comparing the measured integrated intensity to the simulations it follows that the model well describes the actual ripple structure in excellent agreement with the AFM data. From the fit we determined the mean ripple period $\tau = (48 \pm 5)nm$, $\sigma_\tau = (14 \pm 3)nm$, and the shape parameters $R = (19 \pm 5)nm$ and $h_0 = (0.25 \pm 5)nm$. In contrast, the angular map in the other diffraction in Fig. 4(b) does not show any satellites. In this map, the Q_a axis is parallel to the $[\bar{1}10]$ direction, i.e. along the ripples. The surface morphology does not exhibit any pronounced space frequency in this direction

so that no side maxima is observed. From the fact that the intensity distribution along the Q_a axis in Fig. 4 (a) is perfectly symmetric we can argue that the component of the strain parallel to the ripples is either zero or it does not depend on the real-space coordinate along [110], i.e. perpendicular to the ripples. A more substantial GID-based analysis on a variety of (Ga,Mn)As samples will be needed in order to possibly relate the formation of the periodic structures with the presence of uniaxial strain, that may lead to a deeper understanding of the origin of the magnetic anisotropy; this will be the subject of further work.

In conclusion, AFM and X-ray GID measurements have revealed the presence of ripples aligned along the $[1\bar{1}0]$ direction on the surface of (Ga,Mn)As layers grown on GaAs(001) substrates and buffer layers. We find that the strength of the uniaxial anisotropy of these layers increases with the amplitude of the ripples. This suggests that the symmetry breaking uniaxial anisotropy observed in (Ga,Mn)As might be related to these symmetry breaking structural features.

[1] Y. Ohno, D. K. Young, B. Beschoten, F. Matsukura, H. Ohno, and D. D. Awschalom, Nature **402**, 790 (1999).

[2] *Semiconductor Spintronics and Quantum Computation*, edited by D.D. Awschalom, N. Samarth, and D. Loss (Springer, Heidelberg, 2002)

[3] M. Abolfath, T. Jungwirth, J. Brum, and A. H. MacDonald, Phys. Rev. B **63**, 054418 (2001).

[4] J. Zemen, J. Kucera, K. Olejnìk, and T. Jungwirth, Phys. Rev. B **80**, 155203 (2009).

[5] M. Sawicki, K.-Y. Wang, K. W. Edmonds, R. P. Campion, C. R. Staddo, N. R. S. Farley, C. T. Foxon, E. Papis, E. Kaminska, A. Piotrowska, T. Dietl, and B. L. Gallagher, Phys. Rev. B **71**, 121302(R) (2005); K.-Y. Wang, M. Sawicki, K. W. Edmonds, R. P. Campion, S. Maat, C. T. Foxon, B. L. Gallagher, and T. Dietl, Phys. Rev. Lett **95**, 217204 (2005).

[6] D. Hrabovsky, E. Vanelle, A. R. Fert, D. S. Yee, J. P. Redoules, J. Sadowski, J. Kanski, and L. Ilver, Appl. Phys. Lett. **81**, 2806 (2002); H. X. Tang, R. K. Kawakami, D. D. Awschalom, and M. L. Roukes, Phys. Rev. Lett. **90**, 107201 (2003); X. Liu, Y. Sasaki, and J. K. Furdyna, Phys. Rev. B **67**, 205204 (2003); M. Sawicki, F. Matsukura, A. Idziaszek, T. Dietl, G. M. Schott, C. Ruester, C. Gould, G. Karczewski, G. Schmidt, and L. W. Molenkamp, Phys. Rev. B **70**, 245325 (2004).

[7] J. Wunderlich, A. C. Irvine, J. Zemen, V. Holý, A. W. Rushforth, E. De Ranieri, U. Rana, K. Výborný, J. Sinova, C. T. Foxon, R. P. Campion, D. A. Williams, B. L. Gallagher, and T. Jungwirth, Phys. Rev. B **76**, 054424 (2007); J. Wenisch, C. Gould, L. Ebel, J. Storz, K. Pappert, M. J. Schmidt, C. Kumpf, G. Schmidt, K. Brunner, and L. W. Molenkamp, Phys. Rev. Lett. **99**, 077201 (2007); A. W. Rushforth, E. De Ranieri, J. Zemen, J. Wunderlich, K. W. Edmonds, C. S. King, E. Ahmad, R. P. Campion, C. T. Foxon, B. L. Gallagher, K. Výborný, J. Kučera, and T. Jungwirth, Phys. Rev. B **78**, 085314 (2008).

[8] U. Welp, V. K. Vlasko-Vlasov, A. Menzel, H. D. You, X. Liu, J. K. Furdyna, and T. Wojtowicz, Appl. Phys. Lett. **85**, 260 (2004).

[9] G. Apostolopoulos, J. Herfort, L. Däweritz, and K. H. Ploog , Phys. Rev. Lett. **84**, 3358 (2000).

[10] U. Pietsch, V. Holý, and T. Baumbach, *High-Resolution X-Ray Scattering From Thin Films to Lateral Nanostructures*, Springer-Verlag, Heidelberg (2004).

[11] A. Biermanns, U. Pietsch, J. Grenzer, A. Hanisch, S. Facsko, G. Carbone, and T. H. Metzger, J. Appl. Phys. **104**, 044312 (2008).

[12] J. Stangl, V. Holý, and G. Bauer, Rev. Mod. Phys. **76**, 725-783 (2004).